Preprints of the 19th World Congress
The International Federation of Automatic Control
Cape Town, South Africa. August 24-29, 2014

Optimizing Diesel Production Using Advanced Process Control and Dynamic Simulation

Márcio R. S. Garcia * **Renato N. Pitta** ** **Gilvan G. Fischer** **
Enéas R. N. Neto **

* *Radix Engenharia e Desenvolvimento de Software Ltda, Rio de Janeiro, RJ Brazil (e-mail: marcio.garcia@radixeng.com.br)*
** *Refinaria Henrique Lage, São José dos Campos, SP Brazil (e-mail: renato.pitta@petrobras.com.br, gilvan@petrobras.com.br, eneasnascimento@petrobras.com.br)*

Abstract: This paper describes the economical and operational benefits achieved with the use of advanced process control techniques and dynamic simulation applied to a Naphtha Splitter Column. The project consists in optimizing the Diesel blending system of Henrique Lage Refinery (REVAP) located in the state of São Paulo, Brazil. The control strategy was designed to maximize production rate, respecting the operational constraints. The results include an increase in the Naphtha flow stream to the Diesel blending system and improvement of the operational stability, leading to valuable economic gains. The project is also a step forward in the use of Dynamic simulation for modelling and identification, where the simulation models have shown to be representative for the inferential variables integration, adding value to the final result.

Keywords: Advanced Process Control; Optimization, Dynamic Simulation, Naphtha Splitter, Distillation.

1. INTRODUCTION

The use of advanced process control (APC) strategies in the industry has consistently increased in the past few decades and became common practice among those willing to extract all the economic potential of the process, [Delaney, 2012]. Although maximizing their products yields seems to be the primary objective, it is clear that these projects also improve the process safety and operational continuity, among other potential benefits, [Nello, 2011]. Part of the APC success is credited to the evolution of hardware robustness, computational efficiency and software development presented in commercial packages that make possible the implementation of more sophisticated and complex model-based control algorithms. Despite all its potential, it is mandatory to pay special attention to the operational staff's training, [King, 2012] and some other important issues, such as model representability in order to avoid the APC project failure, [Lodolo et al., 2012].

Dynamic simulation is a powerful instrument with modelling capabilities that have been recently adopted by control engineering practitioners. It has given engineers the opportunity to validate new control strategies, obtain dynamic models for inferential variables, supply valuable information for hazop analysis, economical studies report and give assistance during operators training. Virtual plants make possible to study the plant behavior over different scenarios [Al-Dossary et al., 2008], including those undesirable ones where the real plant should not go, [Blevins et al., 2003], [Mansy et al., 2002]. This represents a large improvement on the system's overall reliability, [Luyben, 2012].

This paper presents an application that shows the advantages of combining APC strategies and Dynamic simulation for optimizing a Diesel blending system in a large Brazilian refinery. The APC was designed for maximizing Naphtha addition in the blending system as it handles the Diesel product's flash point. The result is an economic gain associated to the conversion of Naphtha in Diesel, which represents a higher value product, [Kelly and Mann, 2003], [Campos et al., 2013] . The process is detailed in section 2. Section 3 discusses the optimization issues considered for the unit and the benefits of using dynamic simulation for modelling and identification. Section 4 presents some results regarding economical achievements and operational improvements reached by the implemented APC. A conclusion is given to summarize the questions raised throughout the paper and add some perspectives for further improvements.

2. PROCESS DESCRIPTION

The REVAP's Diesel blending system consists of three intermediate products streams: The Diesel streams from the Coker Gasoil Hydrotreating Unit (HDT-GOK) and the Diesel Hydrotreating Unit (HDT-D) and the Heavy Naphtha stream from the Naphtha Splitter Column. These three streams are blended to compose the refinery's Diesel product that is sent to storage. This product must meet the national petroleum agency specifications for certification and commercialization. Otherwise, it is sent for

reprocessing, which represents large economic losses for the refinery. The Naphtha addition lowers the Diesel's flash point and its flow is limited in order to avoid off-specification. The Diesel blending system is illustrated in Fig. 1

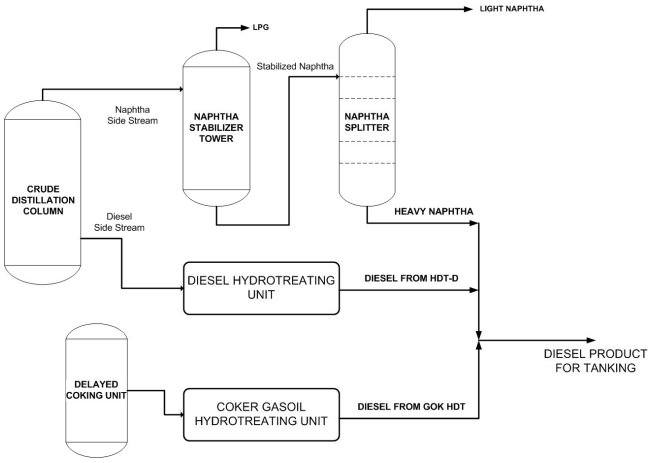

Fig. 1. Diesel blending system.

The Naphtha splitter Column is illustrated in Fig. 2. The inlet stream is composed by the Stabilized Naphtha that comes from the Stabilizer Column of the Crude Distillation Unit. The Splitter's sensitive plate temperature is controlled by the heat exchange between medium pressure steam and the column's side reflux. The top reflux is composed by the Light Naphtha from the top separator vessel and the excess is exported as Petrochemical Naphtha. The column's bottom flow is composed by the Heavy Naphtha, which is added to the Diesel blending system. Since Diesel has a higher economic value when compared to Naphtha and the column's top stream adds no economic value, the economic yields are proportional to the Heavy Naphtha stream that is sent to the Diesel.

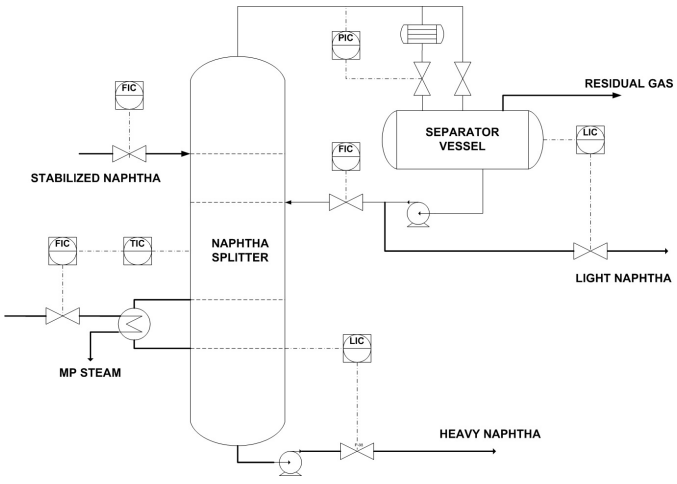

Fig. 2. Naphtha Splitter.

3. OPTIMIZATION

The optimization project of the Naphtha Splitter Column consists in maximizing the processed feed and the Heavy Naphtha flow, which means increasing the refinery's Diesel production. The optimizer is designed to compensate the effects of changes in the feed composition to keep the controlled variables inside the operational range. Also, the lack of on-line and off-line analysers leads to the need of estimating the Heavy Naphtha's flash point. The optimization's objectives were reached through the use of advanced process control and dynamic simulation.

3.1 Advanced Process Control

The designed APC is a two-layer optimizer with the stationary layer running a Quadratic Programming (QP) algorithm used for steady-state optimization and constraints handling, generating the targets for the manipulated and controlled variables (MVs and CVs) of the dynamic layer, where the Cutler's *Dynamic Matrix Control* (DMC) algorithm, [Cutler and Ramaker, 1980] is used for targets tracking and disturbance rejection. The two-layer optimization strategy is illustrated in Figure 3. The QP algorithm, [Garcia and Morshedi, 1986] solves the cost function given by equation (1), [Zanin et al., 2007]:

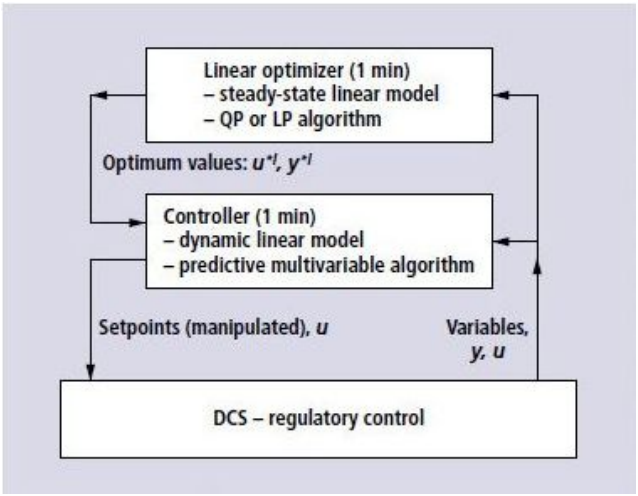

Fig. 3. APC with Two-layer strategy. [Rotava and Zanin, 2005]

$$\min_{\Delta U, SCV} -W_1 \Delta U + \|W_2 \Delta U\|_2^2 + \|W_3 SCV\|_2^2 \quad (1)$$

subject to:

$$\begin{aligned} &\Delta U = U_S - u_{at} \\ &U_S^{inf} \leq U_S \leq U_S^{sup} \\ &Y_S^{inf} \leq Y_S + SCV \leq Y_S^{sup} \end{aligned}$$

where $W_1 = diag[\frac{\partial f_{eco}}{\partial u_1}, \frac{\partial f_{eco}}{\partial u_2}, \ldots, \frac{\partial f_{eco}}{\partial u_n}]$ is the diagonal matrix of the economic coefficients of the manipulated variables (MVs), W_2 is the diagonal matrix of the suppression factors of the MVs and W_3 is the diagonal matrix of weights for the *slack* variables (SCV) used for constraints softening. These three matrices are, in fact, the tuning parameters of the optimization layer. The steady-state optimization uses a linear economic function, thus the W_1 coefficients are constants and they are related to the economic yield achieved with the increment / decrement of the associated MV. U_S is the vector of MVs steady-state targets, u_{at} is the previous control action, U_S^{sup} and

U_S^{inf} are, respectively, the upper and lower constraints of the control actions. Y_S is the CVs steady-state targets vector, Y_S^{sup} and Y_S^{inf} are, respectively, the upper and lower constraints of the controlled variables. The dynamic layer receives these calculated targets and runs the multi-variable predictive control (MPC) algorithm for optimal tracking and disturbances rejection, keeping the process within its operational range. The MPC algorithm control law is shown in equation (2), [Rotava and Zanin, 2005]:

$$\min_{\Delta U_i, i=1,\ldots,nl} \sum_{j=1}^{nr} \|W_4(Y_p - Y_l^*)\|_2^2 + \sum_{i=1}^{nl} \|W_5 \Delta U_i\|_2^2 + \sum_{i=1}^{nl} \|W_6 \left(u_{i-1} + \sum_{k=1}^{i} \Delta U_k - u^* \right) \|_2^2 \quad (2)$$

subject to:

$$-\Delta U^{max} \leq \Delta U \leq \Delta U^{max};\ j = 1, \ldots, nl$$
$$u^{inf} \leq u_{i-1} + \sum_{i=1}^{j} \Delta U_i \leq u^{sup};\ j = 1, \ldots, nl$$

where W_4 is the diagonal matrix for the CVs weights, W_5 is the diagonal matrix of the MVs suppression factors and W_6 is the diagonal matrix of the predicted controller outputs weights. These three matrices are the tuning parameters of the dynamic layer. Y_p is the CVs prediction vector, nr is the prediction horizon, nl is the control horizon and u^* and Y_l^* are the targets calculated by the optimization layer.

The Splitter's APC manipulates the economic related variables: The processed feed, the medium pressure steam consumption and the reflux flow. The CVs represent the operational constraints, i.e., the PID controllers output signals and the inferential variables: The Heavy Naphtha's flash point, the Heavy Naphtha / $T5\%$ ratio (RQT5) and the reflux calculated ratio (RR), which are used to evaluate the column's split quality. $T5\%$ refers to the distillation temperature in which 5% of the total volume of Naphtha is recovered from the gaseous state and it is directly related to the Naphtha's initial boiling point. Table 1 lists all APC variables, where the ↑ symbol means direct action and the ↓ symbol means reverse action, giving an insight of the highly multi-variable behaviour of the plant. TIC, LIC and PIC refers to, respectively, temperature, level and pressure PID controllers in the digital control system (DCS).

Table 1. Manipulated and controlled variables.

	MV's		
	Splitter's feed	Steam Flow	Reflux Flow
CV's			
TIC Process Variable	↓	↑	↓
Bottom LIC control signal	↑	↓	↑
PIC control signal		↑	
Naphtha's Flash point	↓	↑	↓
$RQT5$	↑	↓	↑
RR	↓		↑

3.2 System's Modelling and Identification

The Heavy Naphtha's flash point has great influence in the Diesel's blending system. Once there is no direct formula for its calculation, an inferential model was set using the designed correlation function between the flash point and the $T5\%$ and equations (3) and (4):

$$T5\% = A\left(\frac{Q_{TR}}{Q_{HN}}\right) + B\left(\frac{1}{AUX + \left(\frac{1}{T_{HN}+273}\right)} - 273\right) + C\ +\ BIAS \quad (3)$$

with

$$AUX = \left(\frac{R_{gas}}{9124}\right) * LOG\left(\frac{(P_{HN} + 1.033)}{3.058}\right) \quad (4)$$

where Q_{TR} is the top reflux flow, Q_{HN} is the heavy Naphtha flow, T_{HN} is the heavy Naphtha temperature, R_{gas} is the gas universal constant ($R_{gas} = 1.9872 kcal * K^{-1} * mol^{-1}$) and P_{HN} is the heavy Naphtha's pressure. The equation (4) is a direct application of the Antoine vapour pressure equation, [Green and Perry, 1984]. A daily sampling routine was executed to form a data set for the curve fitting of the model constants A, B and C. Figure 4 shows the correlation between the laboratory's data and the inferential model for the Naphtha's $T5\%$.

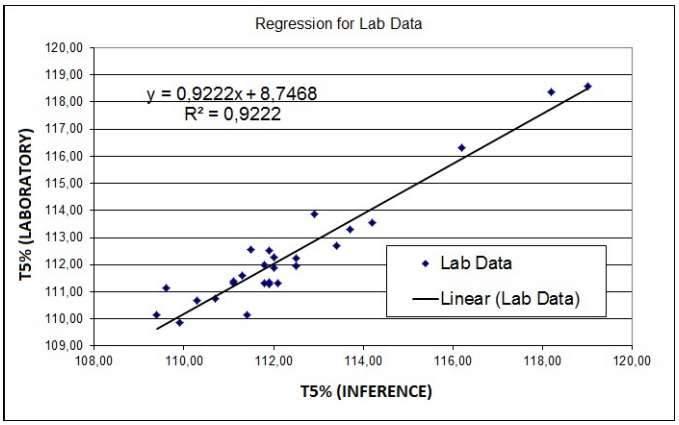

Fig. 4. Curve fitting for Laboratory's T5% data.

The flash point *versus* $T5\%$ correlation function was obtained in the virtual environment through the use of dynamic simulation. The virtual plant was modelled using RSI's Indiss® software, data sheet information and the feed's average split profile given by laboratory analysis. The designed correlation function shown in Figure 5 is a result of tests performed in the virtual plant for different scenarios and steady-state conditions, with the magnitude of the operational variables similar to those of the real plant. The flash point and $T5\%$ values are given by the simulator. The high R^2 fitting factor is an indication of the total correlation between these two variables. Also, the high R^2 factor for the laboratory's $T5\%$ results and the inferential model is also an indication of a proper model approach for the $T5\%$ inference. The Heavy Naphtha flow

/ $T5\%$ ratio and the calculated reflux ration are given by equations (5) and (6).

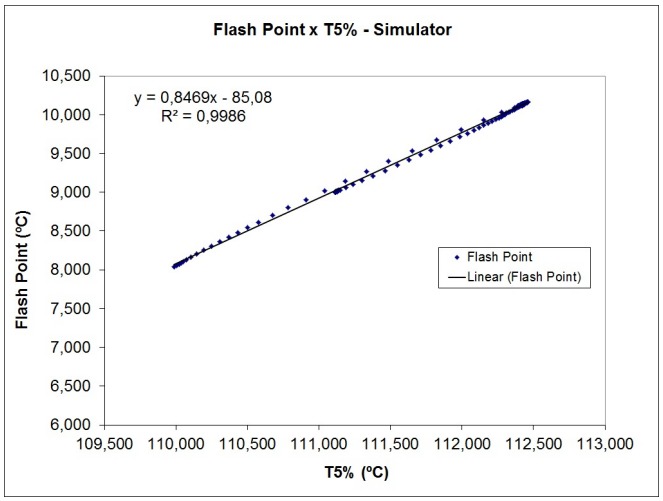

Fig. 5. Curve fitting for Naphtha's flash point.

$$RQT5 = \frac{Q_{HN}}{T5\%} \tag{5}$$

$$RR = \frac{Q_{TR}}{Q_{TR} + Q_{LN}} \tag{6}$$

where Q_{TR} is the top reflux flow, Q_{LN} is the Light Naphtha flow and Q_{HN} is the Heavy Naphtha flow. The *BIAS* parameter in equation (3) is set for data correction based on laboratory's analysis of the flash point for the blended Diesel stream. Since the HDT-GOK's Diesel stream and the blended stream are sampled once per day and the HDT-D Diesel flash point is set to a fixed rate, the Naphtha's flash point can have its *bias* updated using the Hu-Burns mixing rule [Hu and Burns, 1970], given by equations (7) and (8).

$$FPI = \frac{(FP_i + 459.69)^{\frac{1}{X}} * 10^4}{(459.69)^{\frac{1}{X}}} \tag{7}$$

$$FPI_{NS} = \frac{FPI_{DS} * Q_{DS} - FPI_{HDT-D} * Q_{HDT-D}}{Q_{NS}} \tag{8}$$

where FPI is the flash point index for the blended Diesel stream, FP_i is the flash point, in ^oF, for the blended Diesel stream, FPI_{NS} is the flash point index for the Naphtha Splitter stream, FPI_{DS} is the flash point index for the combined Naphtha Splitter and HDT-D streams, Q_{NS} is the Splitter's Heavy Naphtha flow and Q_{DS} is the combined flow of the Splitter and HDT-D streams. The FPI_{DS} can be calculated recursively using the same equations, given that the blended Diesel and the Gasoil HDT Diesel flash points are known. X is a curve fitting parameter and ranges from $-0.025 < X < -0.16$. The FPI_{NS} can be used in equations (9) and (10) to return the Naphtha's flash point, in ^oC.

$$P_{ra} = 459.67 * \left(\frac{FPI_{NS}}{k_1}\right)^{k_2} \tag{9}$$

$$P_c = \frac{P_{ra}}{1.8} - 273.15 \tag{10}$$

where P_{ra} is the flash point in ^oRa, P_c is the Naphtha's flash point in ^oC, k_1 and k_2 are curve fitting parameters. The REVAP's APC project parameters for the Naphtha's flash point inferential model are listed in Table 2.

Table 2. Parameters values for APC project.

Parameter	A	B	C	k_1	k_2	X
Value	9.44	0.7045	−3.7463	10^4	−0.038	−0.06

The identification step tests to obtain the DMC's ARX (***A**uto **R**egressive with e**X**ogenous signal*) models were performed in both real and virtual plants. The tests in the virtual plant were performed to model the controlled variables that, due to the nature of the tests in the real plant, did not present proper response. The data set collected by the virtual plant presents a better signal to noise ratio and is not susceptible to operational disturbances. Also, larger steps can be set to evaluate local non-linearities. The ARX models were obtained for a time sample $T_S = 1$min and a first-order plus dead time (FOPDT) approach.

Figures 6 and 7 show the step response models of both real and virtual plants taken for the $T5\%$ inference and Splitter's temperature. The model validation tests were performed in the real plant environment. One may notice that there is a high correlation between the virtual plant models and the real plant results. For the $T5\%$ inference, the virtual plant model returned a $R^2 = 0.972$ against an almost identical $R^2 = 0.976$ for the real plant model. On the other hand, the virtual plant model for temperature presented a better result, with a $R^2 = 0.987$ against the $R^2 = 0.968$ of the real plant model.

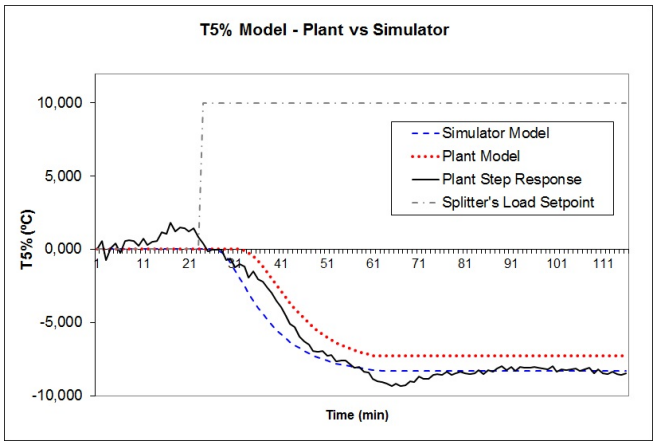

Fig. 6. Virtual Plant vs Real Plant $T5\%$ Model.

Also, it is noticeable that in some cases the real plant models present a steady-state gain error which is caused by uncontrolled disturbances during the step tests or correlated noise that is not sufficiently removed in the identification software. Since the virtual plant models are not susceptible to these disturbances, they sometimes present more consistent results.

Table 3 details the R^2 number for the main controlled variables and the manipulated variables of the APC project,

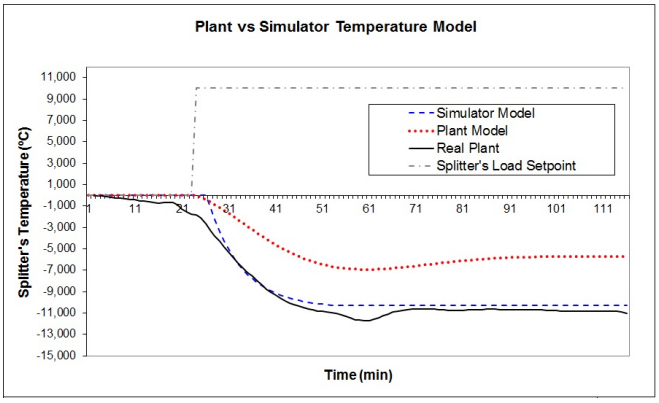

Fig. 7. Virtual Plant vs Real Plant Temperature Model.

where *PLT* refers to real plant based models and *SIM* refers to the virtual plant based models. The dynamic simulator presents better results for some models and very close results for some others. This result validates the designed dynamic simulator turning it into a powerful tool for a more advanced model analysis and the APC tuning tests.

Table 3. Curve fitting factors for the real and virtual plant models.

	Manipulated variable					
	Splitter's Feed		Steam flow		Reflux flow	
Main CV	PLT	SIM	PLT	SIM	PLT	SIM
Splitter's Temperature	0.968	0.987	0.872	0.842	0.948	0.893
LIC Output signal	0.886	0.905	0.750	0.529	0.657	0.737
T5%	0.976	0.972	0.611	0.657	0.862	0.861

4. RESULTS

The Figures 8, 9, 10 and 11 illustrate the performance of the Splitter before and after the APC commissioning for an one-year data set. The results express a considerable increase in the refinery's yields following the maximization of the daily-average flow of Heavy Naphtha and the total processed feed. The APC was commissioned with a prediction horizon $nr = 60$min and control horizon $nl = 8$min, with a time sampling $T_S = 1$min.

Figure 8 shows the increase of the daily-average Heavy Naphtha flow and the six-month average line before and after the APC commissioning. Before the APC project, the Splitter's temperature was controlled to a fixed setpoint, which represented a hard constraint for the operational optimization. The more flexible APC's band control strategy, in counterpart to the regulatory target control, adds up one more degree of freedom, which is used to maximize the processed feed. Figure 9 shows the daily-average processed feed and the six-moth average line before and after the APC commissioning, consolidating the control strategy.

Figure 10 shows the daily average split before and after the APC startup. The APC increased the split profile in 4%, resulting in more extraction of the heavier fractions. This explains why the heavy Naphtha flow is kept on its maximum even if the average processed feed decreases, as seen on Figures 8 and 9.

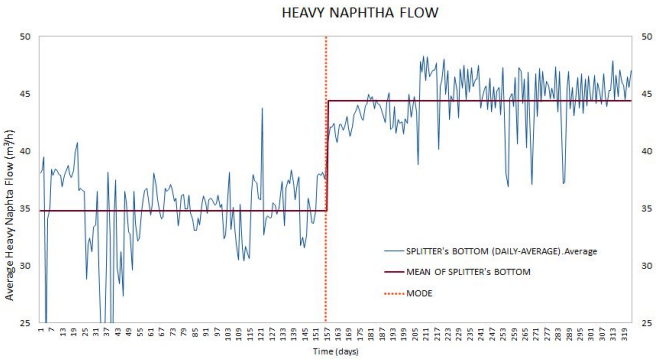

Fig. 8. Heavy Naphtha flow before and after APC.

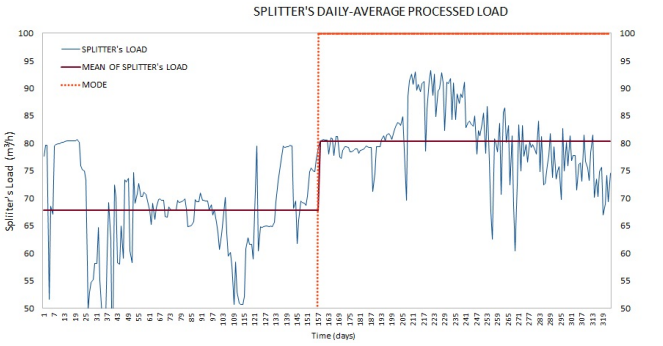

Fig. 9. Stripper's feed before and after APC.

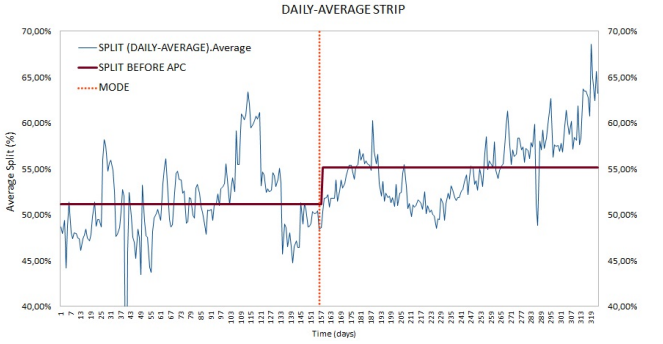

Fig. 10. Daily-average strip before and after APC.

Figure 11 shows the daily average Light Naphtha and Heavy Naphtha flow and also their six-month average line before and after the APC startup. One can see that for a near 50% split both stream are very close in magnitude. The difference between both streams have considerably increased, which resulted in more Naphtha blended into Diesel. It is also noticeable that even if the processed feed decreases for some periods, as seen on Figure 9, this reduction is mainly transmitted to the light Naphtha stream while the heavy Naphtha is kept optimized, due, mainly, to the manipulation of the medium pressure steam flow and the reflux flow.

The calculated data results support the graphic evaluation of the APC's performance. Table 4 shows the average of the three main variables taken into account for the economic-based analysis of the project in a data range of six months before and after the APC commissioning.

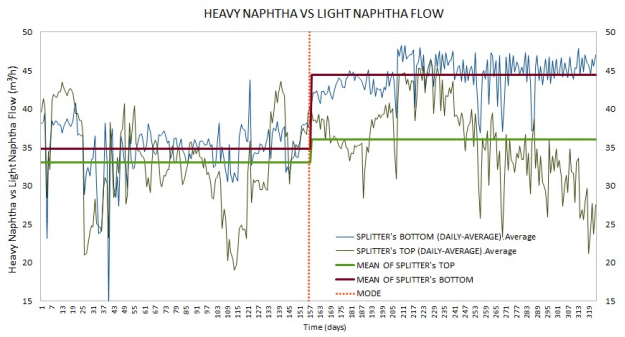

Fig. 11. Light vs Heavy Naphtha flow before and after APC.

Table 4. Unit's performance before / after APC.

	Before APC	After APC	Δ
Processed feed	$67.27m^3/h$	$80.49m^3/h$	19.64%
Heavy Naphtha flow	$34.65m^3/h$	$44.79m^3/h$	29.27%
MP Steam / Feed ratio	$88.73kg/m^3$	$93.96kg/m^3$	5.90%
Split	51.33%	55.61%	8.33%

The average processed feed increased in 19.64% while the Heavy Naphtha flow presented a 29.27% increase on its magnitude. A deeper data analysis shows that in the six months before the APC startup the daily-average processed feed reached the after APC average for only six days. The column's split has also increased in 8.33%. The medium pressure steam consumption / feed ratio represents the necessary steam flow in kg/m^3 of processed feed. Although it has increased, this is necessary since the maximization of the feed is a priority compared to the minimization of the steam consumption as the first one has a higher economic value. The APC project's economic yield can be calculated using equation (11):

$$E = \left(G_1 * \Delta\bar{Q}_{HN} + G_2 * \Delta\bar{Q}_{STEAM}\right) * T_{ON} \qquad (11)$$

where G_1 is the price difference between Diesel and Naphtha in USD/m^3, G_2 is the cost of the medium pressure steam in USD/ton, $\Delta\bar{Q}_{HN}$ is the daily average difference between the Heavy Naphtha flow after and before the APC startup, in m^3/day, $\Delta\bar{Q}_{STEAM}$ is the daily-average difference between the medium pressure steam flow after and before the APC startup, in ton/day and T_{ON} is the time percentage for which the APC is switched on. Based on the results presented in Table 4 and considering the average for the prices in the evaluated period the estimated profit for the APC project is $USD\ 15,700/day$, approximately $USD\ 5,200,000/year$ for an average 91.76% time percentage of T_{ON}.

5. CONCLUSION

The paper results illustrate the economic benefits of the design and implementation of advanced control strategies applied to a Diesel blending system. These benefits come from the incorporation of the heavy Naphtha stream into a higher economic value product. The APC is designed to maximize the Naphtha blending, which is constrained by the Diesel's final flash point while keeping the Splitter's control variables inside the desired operational range. A dynamic simulator was used to develop an inferential model for the flash point and also for the system's identification and control strategy evaluation, giving consistent results for the APC project.

Future improvements include the design and programming of a real-time optimizer in the control algorithm that calculates the blended Diesel flash point based on mixing rules and then returns the minimum limit for the Naphtha's flash point band control. These optimizer is expected to eliminate the need for operator's intervention in order to avoid off-specification of the Diesel properties.

REFERENCES

A. Al-Dossary, M. Al-Juaid, C. Brusamolino, R. Meloni, V. Mertzanis, and V. Harismiadis. Optimize plant performance using dynamic simulation. *Hydrocarbon Processing*, may 2008.

T. E. Blevins, G. K. McMillan, W. K. Wojsznis, and M. W. Brown. *Advanced Control Unleashed*. Number ISBN 1-55617-815-8. ISA-The Instrumentation, Systems,, and Automation Society, 1st edition, 2003.

M. C. M. M. Campos, M. V. C. Gomes, and J. M. G. T. Perez. *Controle Avançado e Otimização na Indústria do Petróleo*. Number ISBN 85-212-0398-5. Interciência, São Paulo, 1st edition, 2013.

C. R. Cutler and D. L. Ramaker. Dynamic matrix control - a computer control algorithm. In *Joint Automatic Control Conference*, 1980.

M.C. Delaney. Advanced process control: A historical perspective. *Process Control and Instrumentation*, pages 89–91, february 2012.

C. E. Garcia and A. M. Morshedi. Quadratic programming solution of dynamic matrix control (qdmc). *Chemical Engineering Communications*, 46:73–87, 1986.

D. W. Green and R. H. Perry. *Perry's Chemical Engineers' Handbook*. McGraw-Hill Professional, 6th edition, 1984.

J. Hu and A. Burns. Index predicts cloud, pour and flash points of distillates fuel blends. *Oil and Gas Journal*, 68:45–66, 1970.

J. D. Kelly and J. L. Mann. Crude-oil blend scheduling optimization: an application with multimillion dollar benefits - part 1. *Hydrocarbon Process*, pages 47–53, 2003.

M.J. King. Why don't we properly train control engineers? *Hydrocarbon Processing*, pages 47–49, october 2012.

S. Lodolo, M. Harmse, A. Esposito, and A. Autuori. Use adaptive modelling to revamp and maintain controllers. *Hydrocarbon Processing*, pages 37–45, june 2012.

W.L. Luyben. Use of dynamics simulation for reactor safety analysis. *Computers and Chemical Engineering*, (40):97–109, February 2012.

M. M. Mansy, G. K. McMillan, and M. S. Sowell. Step into the virtual plant. *Chemical Engineering Progress*, pages 56–61, 2002.

R. Di Nello. Use advanced process control to add value for your facility. *Hydrocarbon Processing*, pages 95–98, june 2011.

O. Rotava and A.C. Zanin. Multivariable control and real-time optimization an industrial practical view. *Hydrocarbon Processing*, pages 61–71, june 2005.

A.C. Zanin, L.F.L. Moro, G. Pinto, and M. Santos. *Curso Sicon10*. Petrobras, 2007.